An MPC/Hybrid System Approach to Traction Control

Francesco Borrelli, Alberto Bemporad, Michael Fodor, and Davor Hrovat

***Abstract*—This paper describes a hybrid model and a model predictive control (MPC) strategy for solving a traction control problem. The problem is tackled in a systematic way from modeling to control synthesis and implementation. The model is described first in the Hybrid Systems Description Language to obtain a mixed-logical dynamical (MLD) hybrid model of the open-loop system. For the resulting MLD model, we design a receding horizon finite-time optimal controller. The resulting optimal controller is converted to its equivalent piecewise affine form by employing multiparametric programming techniques, and finally experimentally tested on a car prototype. Experiments show that good and robust performance is achieved in a limited development time by avoiding the design of ad hoc supervisory and logical constructs usually required by controllers developed according to standard techniques.**

***Index Terms*—Antiskid systems, hybrid systems, model predictive control, multiparametric programming, optimal control, traction control.**

I. Introduction

FOR more than a decade, advanced mechatronic systems controlling some aspects of vehicle dynamics have been investigated and implemented in production [17], [19]. Among them, the class of traction control problems is one of the most studied. Traction controllers are used to improve a driver's ability to control a vehicle under adverse external conditions such as wet or icy roads. By maximizing the tractive force between the vehicle's tire and the road, a traction controller prevents the wheel from slipping and at the same time improves vehicle stability and steerability. In most control schemes the wheel slip, i.e., the difference between the normalized vehicle speed and the speed of the wheel, is chosen as the controlled variable. The objective of the controller is to maximize the tractive torque while preserving the stability of the system. The relation between the tractive force and the wheel slip is nonlinear and is a function of the road condition [2]. Therefore, the overall control scheme is composed of two parts: a device that estimates the road surface condition and a traction controller that regulates the wheel slip at desired values. Regarding the second part, several control strategies have been proposed in the literature mainly based on sliding-mode controllers, fuzzy logic, and adaptive schemes [2]–[4], [21], [22], [25]–[27]. Such control schemes are motivated by the fact that the system is nonlinear and uncertain.

The presence of nonlinearities and constraints on one hand, and the simplicity needed for real-time implementation on the other, have discouraged the design of optimal control strategies for this kind of problem. Recently, we proposed a new framework for modeling hybrid systems [9] and an algorithm to synthesize piecewise linear (indeed, piecewise affine) optimal controllers for such systems [11], [12]. In this paper, we describe how the hybrid framework [9] and the optimization-based control strategy [12] can be successfully applied for solving the traction control problem in a systematic way. The Hybrid Systems Description Language (HYSDEL) [29] is first used to describe a linear hybrid model of the open-loop system suitable for control design. Such a model is based on a simplified model and a set of parameters provided by Ford Research Laboratories, and involves piecewise linearization techniques of the nonlinear torque function that are based on hybrid system identification tools [16]. Then, an optimal control law is designed and transformed to an equivalent piecewise affine function of the measurements, that is easily implemented on a car prototype. Experimental results show that good and robust performance is achieved. Preliminary simulation results were reported in the conference paper [13].

A mathematical model of the vehicle/tire system is introduced in Section II. The hybrid modeling and the optimal control strategy are discussed in Sections III and V, respectively. In Section VI, we derive the piecewise affine optimal control law for traction control; and in Section IX, we present the experimental setup and the results obtained.

Manuscript received January 22, 2003. Manuscript received in final form September 29, 2005. Recommended by Associate Editor S. Kowalewski.

F. Borrelli was with the Automatic Control Laboratory, ETH-Zurich, CH-8092 Zurich, Switzerland. He is now with Dipartimento di Ingegneria, Università del Sannio, Benevento 82100, Italy (e-mail: borrelli@aut.ee.ethz.ch).

A. Bemporad was with the Automatic Control Laboratory, ETH-Zurich, CH-8092 Zurich, Switzerland. He is now with the Dipartimento di Ingegneria dell'Informazione, University of Siena, 53100 Siena, Italy (e-mail: bemporad@dii.unisi.it).

M. Fodor and D. Hrovat are with Ford Research Laboratories, Dearborn, MI 48124 USA (e-mail: mfodor1@ford.com; dhrovat@ford.com; hrovat@comet.srl.ford.com).

Digital Object Identifier 10.1109/TCST.2005.860527

II. Vehicle Model

The simplest model of the vehicle used for the design of the traction controller is depicted in Fig. 1 and consists of the equations

$$\begin{pmatrix} \dot{\omega}_e \\ \dot{v}_v \end{pmatrix} = \begin{pmatrix} -\frac{b_e}{J'_e} & 0 \\ 0 & 0 \end{pmatrix} \begin{pmatrix} \omega_e \\ v_v \end{pmatrix} + \begin{pmatrix} \frac{1}{J'_e} \\ 0 \end{pmatrix} \tau_c + \begin{pmatrix} -\frac{1}{J'_e g_r} \\ \frac{1}{m_v r_t} \end{pmatrix} \tau_t \tag{1}$$

with

$$\tau_c(t) = \tau_d(t - \tau_f) \tag{2}$$

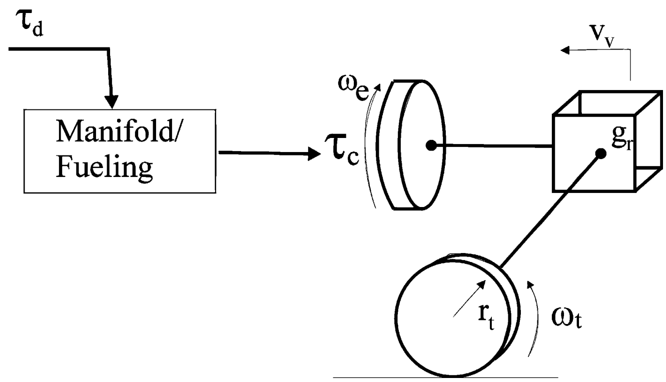

Fig. 1. Simple vehicle model.

TABLE I
PHYSICAL QUANTITIES AND PARAMETERS OF THE VEHICLE MODEL

ω_e	Engine speed
r_t	Tire radius
v_v	Vehicle speed
τ_c	Actual combustion torque
J'_e	Combined engine/wheel inertia
τ_d	Desired combustion torque
b_e	Engine damping
τ_t	Frictional torque on the tire
g_r	Total driveline gear ratio between ω_e and v_v
μ	Road coefficient of friction
m_v	Vehicle mass
τ_f	Fueling to combustion pure delay period
$\Delta\omega$	Wheel slip

where the involved physical quantities and parameters are described in Table I.

Model (1) contains two states for the mechanical system downstream of the manifold/fueling dynamics. The first equation represents the wheel dynamics under the effect of the combustion torque and of the frictional torque, while the second one describes the longitudinal motion dynamics of the vehicle. In addition to the mechanical equations (1) the air intake and fueling model (2) also contributes to the dynamic behavior of the overall system. For simplicity, since the actuator will use just the spark advance, the intake manifold dynamics is neglected and the fueling combustion delay is modeled as a pure delay. Both states are indirectly measured through measurements of front and rear wheel speeds: assuming we are modeling a front-wheel-driven vehicle, ω_e is estimated from the speed of the front wheel, while v_v is estimated from the speed of the rear wheel. The slip $\Delta\omega$ of the car is defined as the difference between the normalized vehicle and engine speeds

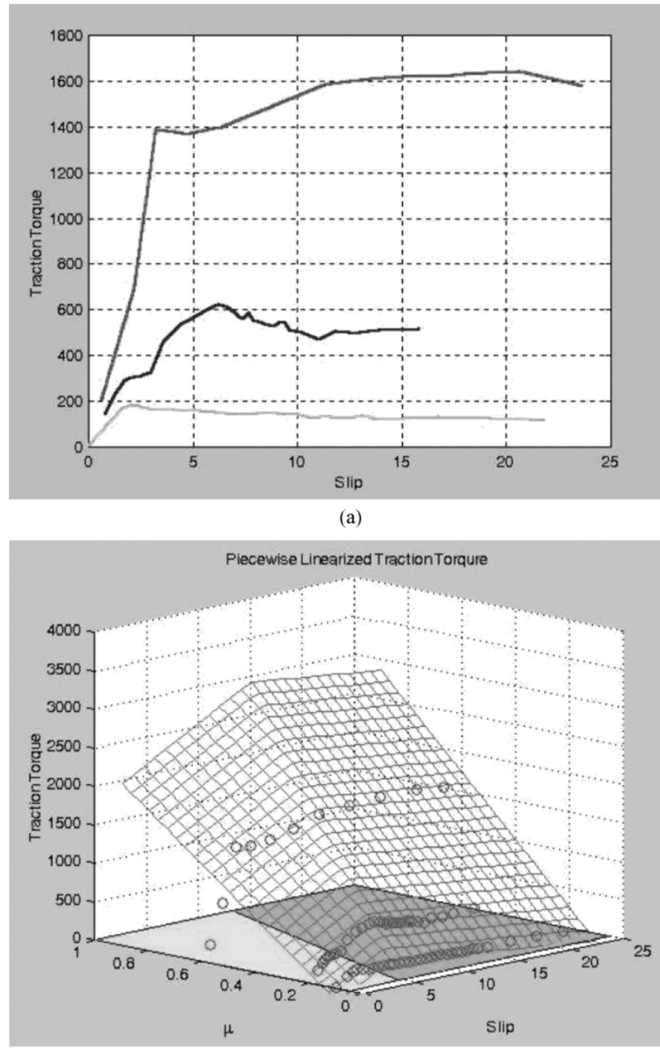

(a)

(b)

Fig. 2. Experimental nonlinear behavior and its piecewise-linear approximation of the frictional torque τ_t as a function of the slip $\Delta\omega$ and road coefficient adhesion μ. (a) Measured tire torque τ_t for three different road conditions: ice (lower plot), snow (middle plot), and concrete (upper plot). (b) Piecewise affine model of the tire torque τ_t. The circles represent measurements data extracted from (a).

$$\Delta\omega = \frac{v_v}{r_t} - \frac{\omega_e}{g_r}. \tag{3}$$

The frictional torque τ_t is a nonlinear function of the slip $\Delta\omega$ and of the road coefficient of friction μ

$$\tau_t = f_\tau(\Delta\omega, \mu). \tag{4}$$

The road coefficient of friction μ depends on the road-tire conditions, while function f_τ depends on vehicle parameters such as the mass of the vehicle, the location of the center of gravity, and the steering and suspension dynamics [25]. Fig. 2(a) shows a typical experimental curve $(\tau_t, \Delta\omega)$ for three different road conditions (ice, snow, and concrete).

Experiments have proven that model (1)–(4) captures the main behavior. In this paper, we will show that it is simple enough to be used for controller design. In literature, the slip $\Delta\omega$ (3) is often normalized such that it assumes values between zero and one; in practice they are both used. In general, the frictional torque τ_t (4) depends on the car's absolute speed. We assume that the effect of the speed variation on the torque can be neglected for the purpose of this paper. In our experiments, the variation of absolute speed is relatively small. We assume that the clutch is locked.

III. Hybrid Systems

Mixed logic dynamical (MLD) systems [9] allow specifying the evolution of continuous variables through linear dynamic equations, of binary variables through propositional logic statements and automata, and the mutual interaction between the two. Linear dynamics are represented as difference equations $x(t+1) = Ax(t) + Bu(t)$, $x \in \mathbb{R}^n$. Boolean variables are defined from linear-threshold conditions over the continuous variables. The key idea of the approach consists of embedding the logic part in the state equations by transforming Boolean variables into 0–1 integers, and by expressing the relations as mixed-integer linear inequalities [9], [14], [24], [30].

By collecting the equalities and inequalities derived from the representation of the hybrid system, we obtain the MLD system [9]

$$x(t+1) = Ax(t)+B_1u(t)+B_2\delta(t)+B_3z(t) \tag{5a}$$

$$E_2\delta(t)+E_3z(t) \le E_1u(t)+E_4x(t)+E_5 \tag{5b}$$

where $x \in \mathbb{R}^{n_c} \times \{0,1\}^{n_\ell}$ is a vector of continuous and binary states, $u \in \mathbb{R}^{m_c} \times \{0,1\}^{m_\ell}$ are the inputs, $\delta \in \{0,1\}^{r_\ell}$, $z \in \mathbb{R}^{r_c}$ represent auxiliary binary and continuous variables, respectively, which are introduced when transforming logic relations into mixed-integer linear inequalities, and A, B_{1-3}, E_{1-5} are matrices of suitable dimensions.

IV. Discrete-Time Hybrid Model of the Vehicle

The model obtained in Section II is transformed into an equivalent discrete-time MLD model through the following steps.

1) The frictional torque τ_t is approximated as a piecewise affine function of the slip $\Delta\omega$ and of the road coefficient of friction μ by using the approach described in [16]. The algorithm proposed in [16] generates a polyhedral partition of the $(\Delta\omega, \mu)$-space and the corresponding affine approximation of the torque τ_t in each region. Alternatively, a similar piecewise affine approximation of the torque function can be computed using the bounded-error approach of [7] to hybrid identification, which allows one to impose a desired maximum approximation error and to determine a corresponding piecewise linear model which fits the data points within such error bound.

   If the number of regions is limited to two, we get

$$\tau_t(\Delta\omega,\mu) = \begin{cases} k_{11}\Delta\omega+k_{12}\mu+k_{13}, & \text{if } 0.21\Delta\omega-5.37\mu\le -0.61 \\ k_{21}\Delta\omega+k_{22}\mu+k_{23}, & \text{if } 0.21\Delta\omega-5.37\mu > -0.61 \end{cases} \tag{6}$$

   where $k_{11} = 67.53$, $k_{12} = 102.26$, $k_{13} = -31.59$, $k_{21} = -1.85$, $k_{22} = 1858.3$, and $k_{23} = -232.51$, as depicted in Fig. 2(b).

2) Model (1) is discretized with sampling time $T_s = 20$ ms and the piecewise affine (PWA) model (6) of the frictional torque is used to obtain the following discrete-time PWA model of the vehicle, as shown in (7) at the bottom of the page, where $\tilde{x} = \left[\begin{smallmatrix}\omega_e\\ v_v\end{smallmatrix}\right]$. At this stage τ_c is considered as the control input to the system. The time delay between τ_c and τ_d will be taken into account in the controller design phase detailed in Section VI-B.

3) The following constraints on the torque, on its variation, and on the slip need to be satisfied:

$$\tau_c \le 176 \text{ Nm} \tag{8a}$$

$$\tau_c \ge -20 \text{ Nm} \tag{8b}$$

$$\dot{\tau}_c \approx \frac{\tau_c(t)-\tau_c(t-1)}{T_s} \le 2000 \text{ Nm/s} \tag{8c}$$

$$\Delta\omega \ge 0. \tag{8d}$$

   In order to constrain the derivative of the input, the state vector is augmented by including the previous torque $\tau_c(t-1)$. The variation of the combustion torque $\Delta\tau_c(t) = \tau_c(t)-\tau_c(t-1)$ will be the new input variable.

We point out here that discrete-time models are needed for recasting the optimal control problem as a mathematical program. The resulting hybrid discrete-time model has three states (x_1 = previous τ_c, $x_2 = \omega_e$, $x_3 = v_v$), one control input ($u_1 = \Delta\tau_c$), one uncontrollable input ($u_2 = \mu$), one regulated

$$\tilde{x}(t+1) = \begin{cases} \begin{bmatrix} 0.98316 & 0.78486 \\ 0.00023134 & 0.989220 \end{bmatrix}\tilde{x}(t) + \begin{bmatrix} 0.048368 \\ 5.6688\text{e}-6 \end{bmatrix}\tau_c(t) \\ \quad + \begin{bmatrix} -0.35415 \\ 0.0048655 \end{bmatrix}\mu(t) + \begin{bmatrix} 0.10943 \\ -0.0015034 \end{bmatrix} & \text{if } 0.21\Delta\omega-5.37\mu \le -0.61 \\ \begin{bmatrix} 1.0005 & -0.021835 \\ -6.4359\text{e}-6 & 1.00030 \end{bmatrix}\tilde{x}(t) + \begin{bmatrix} 0.048792 \\ -1.5695\text{e}-7 \end{bmatrix}\tau_c(t) \\ \quad + \begin{bmatrix} -6.5287 \\ 0.089695 \end{bmatrix}\mu(t) + \begin{bmatrix} 0.81687 \\ -0.011223 \end{bmatrix} & \text{if } 0.21\Delta\omega-5.37\mu > -0.61 \end{cases} \tag{7}$$

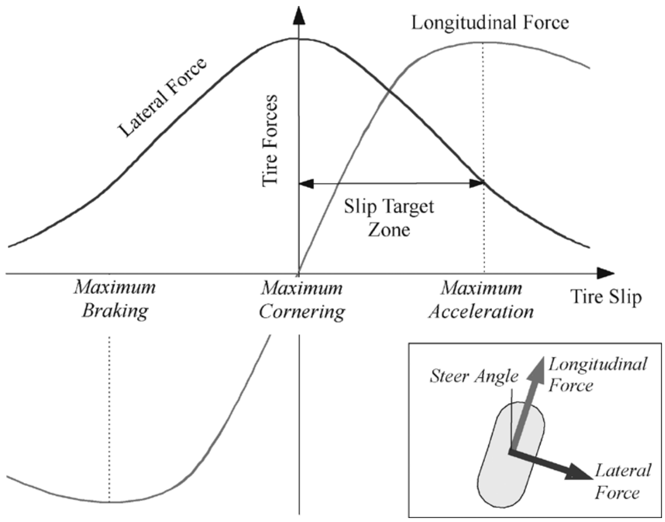

Fig. 3. Typical behavior of lateral and longitudinal tire forces.

output ($y = \Delta\omega$), one auxiliary binary variable $\delta \in \{0, 1\}$ indicating the affine region where the system is operating, $[\delta = 0] \Longleftrightarrow [0.21\Delta\omega - 5.37\mu \leq -0.61]$, and two auxiliary continuous variables $z \in \mathbb{R}^2$ describing the dynamics in (7), i.e.,

$$z = \begin{cases} A_1\tilde{x} + B_{11}\tau_c + B_{12}\mu + f_1, & \text{if } \delta = 0 \\ A_2\tilde{x} + B_{21}\tau_c + B_{22}\mu + f_2, & \text{otherwise} \end{cases}$$

where $A_1, A_2, B_{11}, B_{12}, B_{21}, B_{22}, f_1, f_2$ are the matrices in (7). The resulting MLD model

$$x(t+1) = \begin{bmatrix} 0 & 0 & 0 \\ 0.0484 & 0 & 0 \\ 0.0897 & 0 & 0 \end{bmatrix} x(t) + \begin{bmatrix} 1.0000 & 0 \\ 0.0484 & 0 \\ 0.0897 & 0 \end{bmatrix} \cdot \begin{bmatrix} \Delta\tau_c(t) \\ \mu(t) \end{bmatrix} + \begin{bmatrix} 0 \\ 0 \\ 0 \end{bmatrix} \delta(t) + \begin{bmatrix} 0 & 0 \\ 1 & 0 \\ 0 & 1 \end{bmatrix} z(t) \quad \text{(9a)}$$

$$E_2\delta(t) + E_3 z(t) \leq E_1 \begin{bmatrix} \Delta\tau_c(t) \\ \mu(t) \end{bmatrix} + E_4 x(t) + E_5 \quad \text{(9b)}$$

is obtained by processing the description list reported in the Appendix through the HYSDEL compiler. Matrices $E_1, \ldots, E_5$ include constraints (8); they are omitted here for lack of space and can easily be obtained and analyzed in Matlab using, e.g., the Hybrid Toolbox [5].

V. Constrained Optimal Control

Fig. 3 depicts the lateral and longitudinal frictional torque as a function of the wheel slip. It is clear that if the wheel slip increases beyond a certain value, the longitudinal and lateral driving forces on the tire decrease considerably and the vehicle cannot speed up and steer as desired.

By maximizing the tractive force between the vehicle's tire and the road, a traction controller prevents the wheel from slipping and at the same time improves vehicle stability and steerability. The overall control scheme is depicted in Fig. 4 and is composed of two parts: a device that estimates the road surface condition μ, and consequently generates a desired wheel slip $\Delta\omega_d$, and a traction controller that regulates the wheel slip at the desired value $\Delta\omega_d$. In this paper we only focus on the second part, as the first one is already available from previous projects at Ford Research Laboratories.

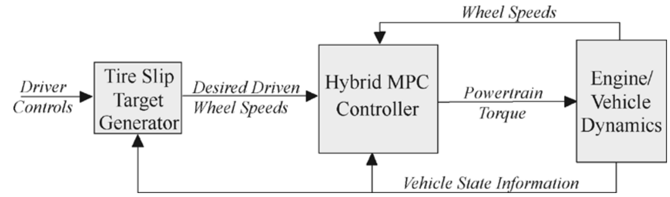

Fig. 4. Overall traction control scheme. In this paper, we focus on the design of the hybrid MPC controller.

The control system receives the desired wheel slip $\Delta\omega_d$, the estimated road coefficient adhesion μ, and the measured front and rear wheel speeds as input, and generates the desired engine torque τ_c (the time delay between τ_c and τ_d will be compensated *a posteriori* as described in Section VI-B).

In the sequel, we describe how a model predictive controller (MPC) can be designed for the posed traction control problem. The main idea of MPC is to use the *model* of the plant to *predict* the future evolution of the system [23]. Based on this prediction, at each time step t, a certain performance index is optimized under operating constraints with respect to a sequence of future input moves. The first of such optimal moves is the *control* action applied to the plant at time t. At time $t+1$, a new optimization is solved over a shifted prediction horizon. For the traction control problem, at each time step t, the following finite horizon optimal control problem is solved:

$$\min_{V} \sum_{k=0}^{T-1} |Q(\Delta\omega_k - \Delta\omega_d(t))| + |R\Delta\tau_{c,k}| \quad (10)$$

$$\text{subj. to} \begin{cases} x_{k+1} = Ax_k + B_1\left[\begin{smallmatrix} \Delta\tau_{c,k} \\ \mu(t) \end{smallmatrix}\right] + B_2\delta_k + B_3 z_k \\ E_2\delta_k + E_3 z_k \leq E_1\left[\begin{smallmatrix} \Delta\tau_{c,k} \\ \mu(t) \end{smallmatrix}\right] + E_4 x_k + E_5 \\ x_0 = x(t) \\ \Delta\tau_{c,k} = \tau_{c,k} - \tau_{c,k-1},\ k = 0, \ldots, T-1, \\ \tau_{c,-1} \triangleq \tau_c(t-1) \end{cases} \quad (11)$$

where matrices $A, B_1, B_2, B_3, E_2, E_3, E_1, E_4, E_5$ are given in (9), $V \triangleq [\Delta\tau_{c,0}, \ldots, \Delta\tau_{c,T-1}]'$ is the optimization vector, and T is the prediction horizon. Note that the optimization variables are the torque variations $\Delta\tau_{c,k} = \tau_{c,k} - \tau_{c,k-1}$, and that the set point $\Delta\omega_d(t)$ and the current road coefficient of adhesion $\mu(t)$ are considered constant over the prediction horizon T.

Equations (10) and (11) can be translated into a mixed integer linear program (MILP) (the minimization of a linear cost function subject to linear constraints with binary and continuous variables) of the form

$$\min_{\mathcal{E},V,Z,\delta} \quad \sum_{k=0}^{T-1} \varepsilon_k^w + \varepsilon_k^u \quad \text{(12a)}$$

$$\text{subject to} \quad G^{\varepsilon}\mathcal{E} + G^u V + G^Z z + G^{\delta}\delta$$

$$\leq S + F \begin{bmatrix} \omega_e(t) \\ v_v(t) \\ \tau_c(t-1) \\ \mu(t) \\ \Delta\omega_d(t) \end{bmatrix} \quad \text{(12b)}$$

where $Z = [z_0', \dots, z_{T-1}']' \in \mathbb{R}^{2T}$, $\delta = [\delta_0, \dots, \delta_{T-1}]' \in \{0,1\}^T$, and $\mathcal{E} = [\varepsilon_0^\omega, \dots, \varepsilon_{T-1}^\omega, \varepsilon_0^u, \dots, \varepsilon_{T-1}^u]' \in \mathbb{R}^{2T}$ is a vector of additional slack variables satisfying $\varepsilon_k^\omega \geq \pm Q(\Delta\omega_k - \Delta\omega_d(t))$, $\varepsilon_k^u \geq \pm R\Delta\tau_{c,k}$, $k = 0, 1, \dots, T-1$ introduced in order to translate the cost function (10) into the linear cost function (12a). Matrices $G^\varepsilon, G^u, G^z, G^\delta, S, F$ are matrices of suitable dimension that, as described in [6], [11], and [12], can be constructed from Q, R, T and $A, B_1, B_2, B_3, E_2, E_3, E_1, E_4, E_5$ (such a construction can be automatically performed by using, for instance, the tool in [5]). The resulting control law is

$$\tau_c(t) = \tau_c(t-1) + \Delta\tau_{c,0}^* \quad (13)$$

where $V^* \triangleq [\Delta\tau_{c,0}^*, \dots, \Delta\tau_{c,T-1}^*]'$ denotes the sequence of optimal input increments computed at time t by solving (12) for the current measurements $\omega_e(t)$, $v_v(t)$, set point $\Delta\omega_d(t)$, and estimate of the road coefficient $\mu(t)$.

VI. Controller Design

The design of the controller is performed in two steps. First, the MPC controller (10)–(13) based on model (9) is tuned in simulation until the desired performance is achieved. The MPC controller is not directly implementable, as it would require the MILP (12) to be solved online at each sampling step, which is clearly prohibitive on standard automotive control hardware. Therefore, for implementation, in the second phase, the explicit piecewise affine form of the MPC law is computed offline by using the multiparametric mixed integer programming (mp-MILP) solver presented in [15]. According to the approach of [11] and [12], the resulting control law has the piecewise affine form

$$\tau_c(t) = F_i\theta(t) + g_i \quad \text{if} \quad H_i\theta(t) \leq k_i,\ i = 1, \dots, n_r \quad (14)$$

where $\theta(t) = [\omega_e(t)\ v_v(t)\ \tau_c(t-1)\ \mu(t)\ \Delta\omega_d(t)]'$. Therefore, the set of states plus references is partitioned into n_r polyhedral cells, and an affine control law is defined in each one of them. Rather than solving the MILP (12) *online* for the given $\theta(t)$, the idea is to use the mp-MILP solver to compute *offline* the solution of the MILP (12) for all the parameters $\theta(t)$ within a given polyhedral set. Although the resulting piecewise affine control action is *identical* to the MPC designed in the first phase, the online complexity is reduced to the simple evaluation of a piecewise affine function. The control law can be implemented online in the following simple way: 1) determine the ith region that contains the current vector $\theta(t)$ (current measurements and references) and 2) compute $\tau_c(t) = F_i\theta(t) + g_i$ according to the corresponding ith control law. A more efficient way of evaluating the piecewise affine control law based on the organization of the controller gains on a balanced search tree is reported in [28].

A. Tuning

The parameters of the controller (10)–(13) to be tuned are the horizon length T and the weights Q and R. By increasing the prediction horizon T, the controller performance improves, but at the same time the number of constraints in (11) increases. As in general the complexity of the final piecewise affine controller increases dramatically with the number of constraints in (11) (see [10] for the case of linear systems), tuning T amounts to finding the smallest T, which leads to a satisfactory closed-loop behavior. Simulations were carried out to test the controller against changes to model parameters. Experimental results and simulations have proven that such horizon is a good compromise between performance and computational complexity. Performance can be improved with longer horizons in simulation, though the model mismatch present on the tire models bound such improvement in experiments. Robustness has been proved with extensive simulations. Theoretical results on robustness of constrained hybrid systems are still under investigation.

A satisfactory performance was achieved with $T=4$, $Q=50$, $R = 1$, which corresponds to an explicit controller consisting of $n_r = 137$ regions. We will refer to this as *hybrid controller*. We have tried also controllers with larger horizons both in simulation and in experiments. We do not include the results in this paper. In order to have a feeling on the sensitivity of the solution complexity to the horizon length, we mention here that by using $T = 5$, $Q = 50$, $R = 1$, one obtains a slightly better performance at the price of $n_r = 504$ regions in the explicit controller.

B. Combustion Torque Delay

The vehicle model in Section II is affected by a time delay of $\sigma = \tau_f/T_s = 12$ sampling intervals between the desired commanded torque τ_d and the combustion torque τ_c. To avoid the introduction of σ auxiliary states in the hybrid model (5), we take such a delay into account only during implementation of the control law.

Let the current time be $t \geq \sigma$ and let the explicit optimal control law in (14) be denoted as $\tau_c(t) = f_{\mathrm{PWA}}(\theta(t))$. Then, we compensate for the delay by setting

$$\tau_d(t) = \tau_c(t+\sigma) = f_{\mathrm{PWA}}\left(\hat{\theta}(t+\sigma)\right) \quad (15)$$

where $\hat{\theta}(t+\sigma)$ is the σ-step ahead predictor of $\theta(t)$. Since at time t, the inputs $\tau_d(t-i)$, $i = 1, \dots, \sigma$, and therefore $\tau_c(t-i+\sigma)$, $i = 1, \dots, \sigma$, are available, $\hat{\theta}(t+\sigma)$ can be computed from $\omega_e(t)$, $v_v(t)$ by iterating the PWA model (7) under the assumption $\mu(t+k) \equiv \mu(t)$, $\forall k = 0, 1, \dots, \sigma$.

In order to motivate the assumption in (15), in the Appendix we show that for the related setting of linear quadratic regulation (LQR) of linear time-invariant models with delays (quadratic performance indexes, infinite prediction horizon), such an assumption is exact, that is, the LQR gain for the delayed system is obtained by combining the LQR gain for the delay-free system with a σ-steps ahead predictor. Through tedious algebraic manipulations, it is possible to prove that this is true also in the present hybrid finite-horizon context.

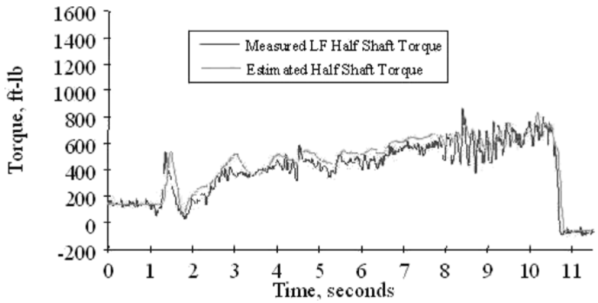

Fig. 5. Measured and estimated half-shaft torque during TC operation.

C. Road-Tire Friction Estimation

An important ingredient of a well-developed traction control system is the ability to estimate the friction coefficient between the road and tire. In the context of the above control system design, this means that it is important to identify what kind of road or ground surfaces the vehicle is traversing, which may include snow, ice, sand, etc. Then, depending on the road/tire friction interface properties, one can chose the appropriate control settings as discussed above.

In general, the tire-road friction estimation algorithms can be loosely grouped in two different classes, depending whether the estimation is focused on the steep-positive-slope or almost-flat portion of the tire tractive force versus slip curve. Some of the most common approaches are based on wheel spins, so that the estimation is performed primarily during the excessive wheel slips or spins on a mostly flat portion of the tire force-slip curve. During these periods, one estimates the wheel torque and corresponding tire tractive force, which is then divided by the normal force to obtain an estimate of the prevailing friction potential. The wheel torque can be estimated using dynamic models of relevant parts of power train, where one can further increase the robustness of the estimate by exploiting different torque paths [20].

One practical example of such an approach is proposed in [1]. The corresponding estimation results in terms of coefficient of friction can be found in [19], for the case of abrupt snow-to-ice transitions. The quality and speed of estimation in this case was facilitated by appropriate wheel torque estimation. Typical performance of the torque estimator used in this paper is shown in Fig. 5, which compares the estimated and actual measured half-shaft torque (closely related to the wheel torque in the present case) during vehicle operation on a split (ice-cement) road surface. Additional details can be found in [19].

For the above estimation approach to work, it was necessary to produce a wheel spin that would guarantee the operation on the near flat portion of the tire force-slip curve. This initial spin then can lead to loss of vehicle tractive performance and directional or handling capacity. In some cases—such as a vehicle coasting down a stretch of slippery road—the initial wheel-spin could be avoided if a timely online estimate of road surface characteristics could be produced even before the abrupt application of a gas pedal. The corresponding estimation techniques are based on the estimation of the prevailing slopes in the initial, steep-positive-slope region of the tire force-slip curves, where slip is typically small (see, e.g., [18]). While such techniques lead to somewhat slower estimation, and are in general less robust, they create opportunities for further significant improvements in traction and overall vehicle control in the future.

Since this paper focuses on model predictive and hybrid aspects of controls, the simulations were run under the assumption that an exact estimate of road friction is available at the start of (but not before) the first spin. However, the actual vehicle tests were performed with a controller that included a practical estimator based on the first approach described above, i.e., based on the near flat portion of the tire force-slip characteristics [1]. Future developments may include the estimators based on the second approach, which can nicely complement predictive capabilities of MPC and hybrid controls.

VII. Motivation for Hybrid Control

There are several reasons that led us to solve the traction control problem by using a hybrid approach. First, the nonlinear frictional torque τ_t in (4) has a clear piecewise-linear behavior [27]: The frictional torque increases almost linearly for low values of the slip, until it reaches a certain peak after which it starts decreasing. For various road conditions the curves have different peaks and slopes. By including such a piecewise linearity in the model, we obtained a single control law that is able to achieve the control task for a wide range of road conditions. Moreover, the design flow has the following advantages.

1) From the definition of the control objective to its solution, the problem is tackled in a systematic way by using the HYSDEL compiler and multiparametric programming algorithms.
2) Constraints are embedded in the control problem in a natural and effective way.
3) The resulting control law is piecewise affine and requires much less supervision by logical constructs than controllers developed with traditional techniques [e.g., proportional-integral-differential (PID) control].
4) It is easy to extend the design to handle more accurate models and include additional constraints without changing the design flow. For example, one can use a better piecewise-linear approximation of the frictional torque, a more detailed model of the dynamics, and include logic constructs in the model such as an hysteresis for the controller activation as a function of the slip.

In terms of performance, the results obtained with our approach are comparable with a well-tuned PID controller used at Ford Motor Company. The experiments will show that a good performance is achieved despite the limited development time compared to the time needed for the design of the PID controller. Moreover, the hybrid approach proposed in this paper provides an insight on the achievable limits of control performance, as discussed next.

VIII. Simulation Results

Extensive simulations were carried out before testing the hybrid controller on a passenger vehicle. In particular, we first consider standard linear MPC design. We consider different controllers, based on linear or affine models of the vehicle. Then, we compare their performance with respect to the hybrid MPC controller performance. In this section, we present a summary of the simulation results obtained by using linear and hybrid MPC synthesis techniques.

The choice of linear prediction models is dictated by well-known experimental results. There is a large qualitative difference in two different regions of slip operations. In the first region the system is stable and the torque increases as a function of the slip (denoted as affine model 1). In the second region, the system is unstable (or marginally stable) and the torque decreases as a function of the slip (affine model 2). By combining (1) and (6), we obtain two linear models for the vehicle dynamics of dimension two

Affine model 1

$$\begin{bmatrix}\dot{\omega}_e\\ \dot{v}_v\end{bmatrix} = \begin{bmatrix}-\frac{b_e}{J'_e}-\frac{k_{11}}{J'_e g_r^2} & \frac{k_{11}}{J_e} g_r r_t\\ \frac{k_{11}}{m_v r_t g_r} & -\frac{k_{11}}{m_v r_t^2}\end{bmatrix}\begin{bmatrix}\omega_e\\ v_v\end{bmatrix} + \begin{bmatrix}\frac{1}{J'_e}\\ 0\end{bmatrix}\tau_c + \begin{bmatrix}-\frac{k_{12}}{J'_e g_r}\\ \frac{k_{12}}{m_v r_t}\end{bmatrix}\mu + \begin{bmatrix}-\frac{k_{13}}{J'_e g_r}\\ \frac{k_{13}}{m_v r_t}\end{bmatrix} \tag{16}$$

Affine model 2

$$\begin{bmatrix}\dot{\omega}_e\\ \dot{v}_v\end{bmatrix} = \begin{bmatrix}-\frac{b_e}{J'_e}-\frac{k_{21}}{J'_e g_r^2} & \frac{k_{21}}{J_e} g_r r_t\\ \frac{k_{21}}{m_v r_t g_r} & -\frac{k_{21}}{m_v r_t^2}\end{bmatrix}\begin{bmatrix}\omega_e\\ v_v\end{bmatrix} + \begin{bmatrix}\frac{1}{J'_e}\\ 0\end{bmatrix}\tau_c + \begin{bmatrix}-\frac{k_{22}}{J'_e g_r}\\ \frac{k_{22}}{m_v r_t}\end{bmatrix}\mu + \begin{bmatrix}-\frac{k_{23}}{J'_e g_r}\\ \frac{k_{23}}{m_v r_t}\end{bmatrix}. \tag{17}$$

The next choice of linear models (denoted as linear model 3 and linear model 4) considers the same two regions of slip operation as before, but it also includes an additional state which is used to estimate the torque τ_t. In fact, by combining (1) and the derivative of τ_t obtained by differentiating (6), we obtain two linear models of dimension three for the vehicle dynamics

Linear model 3

$$\begin{bmatrix}\dot{\omega}_e\\ \dot{v}_v\\ \dot{\tau}_t\end{bmatrix} = \begin{bmatrix}-\frac{b_e}{J'_e} & 0 & -\frac{1}{J'_e g_r}\\ 0 & 0 & \frac{1}{m_v r_t}\\ -\frac{k_{11}J'_e}{g_r b_e} & 0 & -k_{11}J'_e - k_{11}m_v\end{bmatrix}\begin{bmatrix}\omega_e\\ v_v\\ \tau_t\end{bmatrix} + \begin{bmatrix}\frac{1}{J'_e}\\ 0\\ 0\end{bmatrix}\tau_c \tag{18}$$

Linear model 4

$$\begin{bmatrix}\dot{\omega}_e\\ \dot{v}_v\\ \dot{\tau}_t\end{bmatrix} = \begin{bmatrix}-\frac{b_e}{J'_e} & 0 & -\frac{1}{J'_e g_r}\\ 0 & 0 & \frac{1}{m_v r_t}\\ -\frac{k_{21}J'_e}{g_r b_e} & 0 & -k_{21}J'_e - k_{21}m_v\end{bmatrix}\begin{bmatrix}\omega_e\\ v_v\\ \tau_t\end{bmatrix} + \begin{bmatrix}\frac{1}{J'_e}\\ 0\\ 0\end{bmatrix}\tau_c. \tag{19}$$

These four models were used to design four linear MPC controllers subject to constraints (8), where the delay in (2) was compensated as described in Section VI-B. The four linear traction controllers were simulated by using a nonlinear model of the vehicle driving on a polished ice surface ($\mu = 0.2$) with $\omega_e(0) = 180.6$ rad/s and $v_v(0) = 0$ m/s (which represent the vehicle standing initially still with the wheels slipping). We compared the performance of the linear controllers to the one obtained by using a hybrid controller.

Linear MPC based on affine model 1. The performance is in general very bad independently of the MPC tuning. Fig. 6 depicts a simulation of one of the best tuned MPC based entirely on affine model 1. The explanation for such poor behavior can be mainly found in the large model mismatch, due to the large difference in tire slope characteristics between the two model regions. This poor performance may be improved by adding a Kalman filter or, perhaps better, by adding additional states (for instance, by extending the linear two-dimensional model with the integral of the output in order to obtain an integral action, as was done in the hybrid context in [8]). The benefits of using Kalman filtering and of augmenting the linear model with additional states are clear when linear model 3 is used.

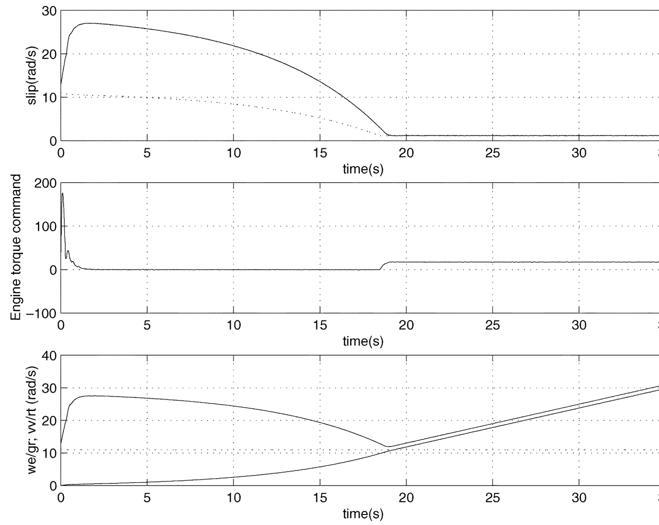

Fig. 6. Simulation results: linear MPC based on affine model 1, $\Delta\omega_d = 2$ rad/s. In the upper plot, the slip trace is a solid line and the desired slip is a dotted line.

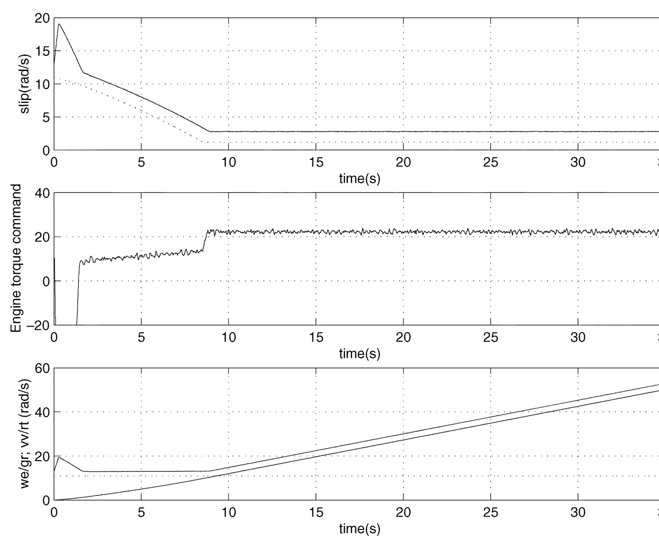

Fig. 7. Simulation results: linear MPC based on affine model 2, $\Delta\omega_d < 2$ rad/s. In the upper plot, the slip trace is a solid line and the desired slip is a dotted line.

Linear MPC based on affine model 2. The performance improves compared to affine model 1. However, a small model mismatch generates a steady-state offset, as can be seen in Fig. 7. Such a steady-state error can be removed with the introduction of additional states and Kalman filtering, as described earlier. The advantage of using Kalman filtering and an extended model is apparent from the performance achieved by using linear model 4.

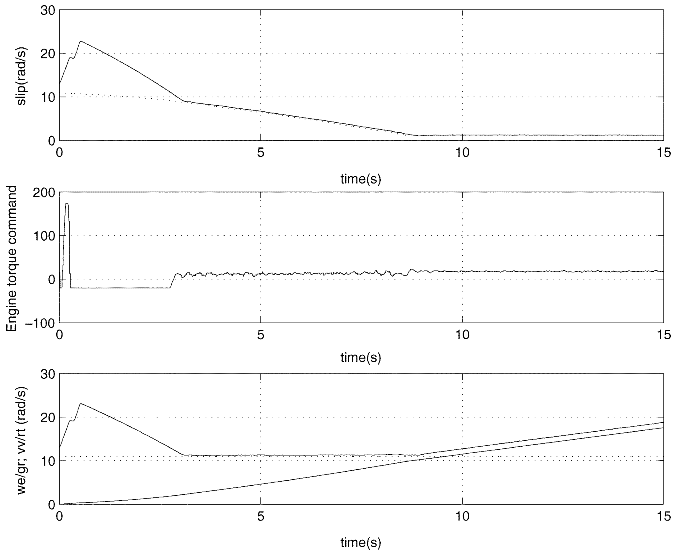

Fig. 8. Simulation results: linear MPC based on linear model 4, $\Delta\omega_d = 2$ rad/s. In the upper plot, the slip trace is a solid line and the desired slip is a dotted line.

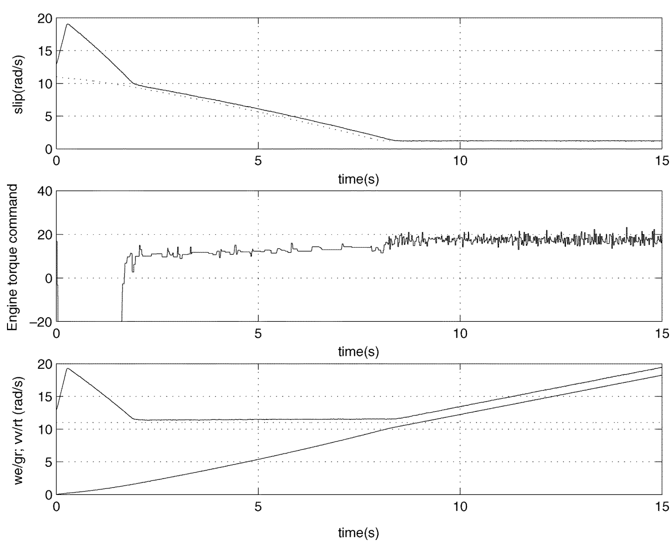

Fig. 9. Simulation results: MPC based on hybrid model, $\Delta\omega_d = 2$ rad/s. In the upper plot, the slip trace is a solid line and the desired slip is a dotted line.

Linear MPC based on linear models 3 and 4. These two cases lead to similar performance, which is, in general, good, as can be seen from Fig. 8 for the case of model 4. In fact, the vehicle model is very sensitive to the frictional torque model τ_t. In models 3 and 4, the frictional torque τ_t is a state that can be estimated from the measurements by using a Kalman filter. Despite a model mismatch, the estimation of τ_t is relatively good, and this justifies the good performance of such controllers.

Hybrid MPC based on MLD model (9). Fig. 9 depicts the simulation results for the hybrid case. The first immediate comparison between the linear MPC and the hybrid MPC can be highlighted. The linear MPC presents about 21% larger initial spin compared to the hybrid MPC; this can be seen by comparing Fig. 8 with the corresponding simulation results for the hybrid case shown in Fig. 9. Note in particular that model 4 leads to an additional engine torque pulse in the initial phase of slip control, which in turn results in an additional "glitch" in the initial slip curve and overall more excessive initial spin.

The experimental results obtained with the linear MPC controller based on model 4 will be presented in the next section. We want to point out that the optimal hybrid controller presented in this paper quantifies the best performance achievable in the control problem at hand, therefore providing a measurement unit for the degree of performance achieved by the linear MPC controllers, which is unknown *a priori*.

IX. Experimental Setup and Results

The hybrid traction controller was tested in a small (1390 kg) front-wheel-drive passenger vehicle with manual transmission. The explicit controller was run with a 20-ms timebase in a 266-MHz Pentium II-based laptop. Vehicle wheel speeds were measured directly by the laptop computer, and the calculated engine torque command was passed to the powertrain control module through a serial bus. Torque control in the engine was accomplished through spark retard, cylinder air/fuel ratio adjustment, and cylinder fuel shutoff where needed. The overall system latency from issuance of the torque command to production of the actual torque by the engine by the engine was relatively large (0.25 s), which is in part attributed to computational and implementation delays. The vehicle was tested on a polished ice surface (indoor ice arena, $\mu \simeq 0.2$) with a variety of ramp, step, and sinusoidal tracking reference signals. Control intervention was initiated when the average driven wheel speed exceeded the reference wheel speed for the first time.

As indicated above, the experiments were conducted on a uniform ice surface in an ice arena that provided suitable test and development facilities during the warmer periods of the year. Due to the obvious space limitations, only limited speed tests were possible, which can still display key characteristics of a given traction control system. In particular, the tests were done for aggressive, wide-open throttle ("full gas") tip-ins from a standstill condition in first gear, where brakes were typically applied prior to the tip-in and the clutch was abruptly and fully engaged. This large initial disturbance and subsequent "pedal-to-the-metal" operation creates some of the most demanding conditions for the traction controller. Note that the target slip is initially step-changed to about 10 rad/s and then gradually lowered as the engine speed is kept constant during the vehicle launch acceleration. Once the vehicle speed reaches the synchronous level with the corresponding engine speed (around 10 s) the slip target is kept to a constant value of 2 rad/s.

Fig. 10 shows test results for the case of a linear MPC based on model 4, and Fig. 11 for the hybrid control case. From the sinusoidal response in Fig. 10(b), it can be seen that the MPC systems bandwidth is around 0.5 Hz. In addition, the comparison of Figs. 10 and 11 show that the hybrid control on the average results in circa 20% lower initial slip peak and significantly faster containment of the first spin. As explained in Section VIII, this is due to an additional engine torque hesitation pulse that can be seen in Fig. 10.

Extensive study of simulations and experimental results have revealed that the oscillations that can be observed in the hybrid

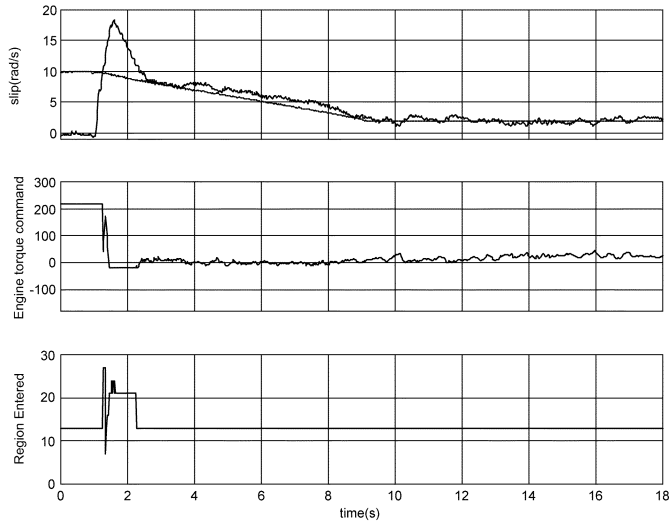

(a)

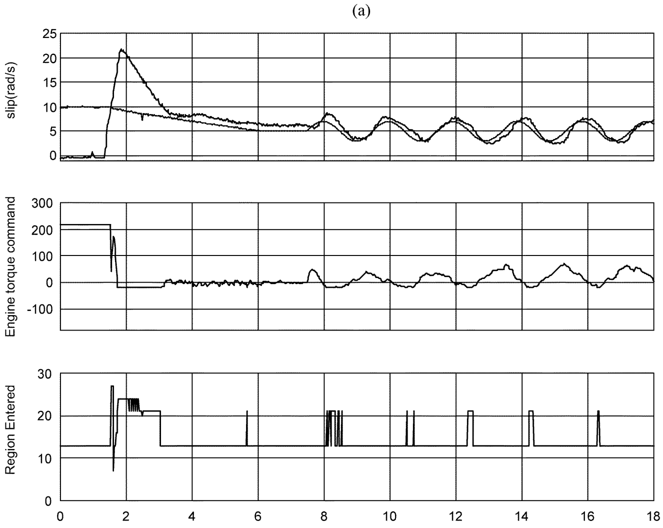

(b)

Fig. 10. Experimental results: linear MPC based on linear model 4. The third and sixth plots depict the operating region i of the explicit controller (14), with $i \leq n_r$. (a) Ramp and step slip reference. (b) Sinusoidal slip reference.

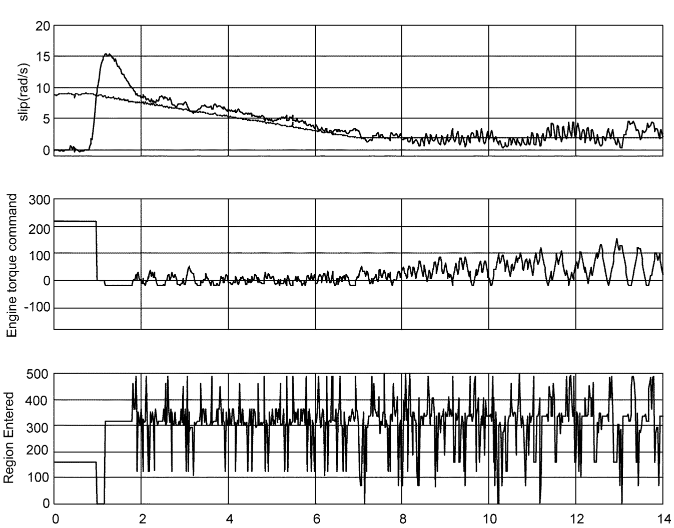

Fig. 11. Hybrid controller. Experimental results for a step slip reference. The third plot depicts the operating region i of the explicit controller (14), with $i \leq n_r$.

case (Fig. 11) are due to the use of absolute values in cost function (10). The oscillations can be reduced by using smoother objective functions based on quadratic errors. The use of explicit hybrid MPC based on quadratic performance is under investigation by the authors. The theory and the results for the case of quadratic costs will be reported in future publications. We want to mention that the frequencies of the oscillations that can be seen in Fig. 11 are filtered by the dynamics of the car; thus, they are typically not felt by the driver.

A comparison between the test results of Figs. 10 and 11 and corresponding simulation results of Figs. 8 and 9 reveals similar trends, including the above hesitation pulse effects and significantly smaller slip overshoots and better overall slip target tracking achieved with the hybrid controller (relatively large initial engine torque of circa 220 Nm is not present in the simulation results, which used an effective net torque between the engine and brakes). Good qualitative and quantitative correlation between the simulation and experimental results confirms that the above simple model was appropriate for this paper.

X. Concluding Remarks

In this paper, we described a hybrid model and an optimization-based control strategy for a vehicle traction control problem. We showed, through experiments carried out at Ford Research Laboratories, that good and robust performance is achieved on polished ice, which represents some of the most challenging road surfaces since it requires the largest amount of torque reduction and precise control in the least favorable (small signal-to-noise ratio) region of vehicle operations. The performance was relatively robust with respect to manual transmission clutch modes of application, which represents a challenging disturbance that is characteristic for manual power trains with their inherent event-to-event and driver-to-driver variability. It was also shown, through a comparison between simulation and actual vehicle test results, that the simple vehicle model used for the study reported in this paper was well suited for MPC and hybrid control designs and related performance predictions. Furthermore, the resulting optimal piecewise affine control law was easily implemented on low-cost testing hardware.

The simulation and test results demonstrated that the l_1-optimal hybrid controller used in this problem can lead to about 20% reduction in peak slip amplitudes and corresponding spin duration when compared to best case linear MPC counterparts. At the same time, the hybrid controller provided a systematic way to create a benchmark of optimal possible performance against which many other controllers—classical as well as modern—could be compared.

It should be pointed out that this paper was based on a very course approximation of tire characteristic curves. Further improvements are possible by more granular resolution of these characteristics. For these more complex piecewise affine partitions, we are developing efficient forms of implementation that greatly reduce the number of regions to be stored by exploiting properties of multiparametric linear programming. We are also currently working to extend the results of this paper to MPC formulation based on quadratic costs.

APPENDIX

Below we report the description list in HYSDEL of the traction control model described in Section IV.

```
SYSTEM FordCar {

INTERFACE {
/* Description of variables and constants */

   STATE {
          REAL taotold;
          REAL we;
          REAL vv;
   }

   INPUT { REAL deltataot; REAL mu;
   }

   PARAMETER {

          /* Region of the PWA linearization */
          /* ar * mu + br * deltaw <= cr */
          REAL ar = -5.3781;
          REAL br = 53.127/250;
          REAL cr = -0.615 32;

          /* Other parameters */
          REAL deltawmax = 400; /
          REAL deltawmin = -400;
          REAL zwemax = 1000;
          REAL zwemin = -100;
          REAL zvvmax = 80;
          REAL zvvmin = -100;
          REAL gr = 13.89;
          REAL rt = 0.298;
          REAL e = 1e-6;

          /* Dynamic behavior of the model
(Matlab generated) */
          REAL a11a = 0.983 16;
          REAL a12a = 0.784 86;
          REAL a21a = 0.000 231 34;
          REAL a22a = 0.989 220;
          REAL b11a = 0.048 368;
          REAL b12a = -0.354 15;
          REAL b21a = 0.089 695;
          REAL b22a = 0.004 865 5;
          REAL f1a = 0.048 792;
          REAL f2a = -1.5695e-007;

          REAL a11b = 1.0005;
          REAL a12b = -0.021 835;
          REAL a21b = -6.4359e-006;
          REAL a22b = 1.000 30;
          REAL b12b = -6.5287;
          REAL b22b = 0.089 695;
          REAL f1b = 0.816 87;
          REAL f2b = -0.011 223;
          }
   }

IMPLEMENTATION {
   AUX {
          REAL zwe, zvv;
          BOOL region;
   }
   AD {
          /* PWA Domain */
          region = ar * ((we/gr) - (vv/rt)) + br *
mu - cr <= 0
[deltawmin, deltawmax, e];
   }
   DA {
       zwe={IF region THEN a11a*we+a12a*
vv + b12a * mu + f1a
[zwemin, zwemax, e]
          ELSE a11b * we + a12b * vv + b12b *
mu + f1b
[zwemin, zwemax, e]
          };
       zvv={IF region THEN a21a*we+a22a*
vv + b22a * mu + f2a
[zvvmin, zvvmax, e]
          ELSE a21b * we + a22b * vv + b22b *
mu + f2b
[zvvmin, zvvmax, e]
   };
          }

CONTINUOUS {
          taotold = deltataot;
          we = zwe + b11a * taotold + b11a *
deltataot;
          vv = zvv + b21a * taotold + b21a *
deltataot;
        }

MUST {deltataot <= 2000;
        taotold <= 176;
        -taotold <= 20;
        (we/gr) - (vv/rt) >= 0;
   }
}
}
```

Consider discrete-time linear system

$$x(t+1) = Ax(t) + Bu(t-\Delta) \tag{20}$$

where $x(t) \in \mathbb{R}^n$ and $u(t) \in \mathbb{R}^m$ are the state and input vectors, respectively, and the corresponding augmented system

$$\tilde{x}(t+1) = \tilde{A}\tilde{x}(t) + \tilde{B}u(t) \tag{21}$$

where

$$\tilde{x}(t) = \begin{bmatrix} x(t) \\ u(t-\Delta) \\ u(t-\Delta+1) \\ \vdots \\ u(t-1) \end{bmatrix} \tag{22}$$

and

$$\tilde{A} = \begin{bmatrix} A & B & \mathbf{0}_{n\times m} & \cdots & \mathbf{0}_{n\times m} \\ \mathbf{0}_{m\times n} & \mathbf{0}_{m\times m} & \mathbf{I}_{m\times m} & \cdots & \mathbf{0}_{m\times m} \\ \vdots & \vdots & \vdots & \vdots & \vdots \\ \mathbf{0}_{m\times n} & \mathbf{0}_{m\times m} & \mathbf{0}_{m\times m} & \cdots & \mathbf{I}_{m\times m} \\ \mathbf{0}_{m\times n} & \mathbf{0}_{m\times m} & \mathbf{0}_{m\times m} & \cdots & \mathbf{0}_{m\times m} \end{bmatrix},$$

$$\tilde{B} = \begin{bmatrix} \mathbf{0}_{n\times m} \\ \mathbf{0}_{m\times m} \\ \vdots \\ \mathbf{0}_{m\times m} \\ \mathbf{I}_{m\times m} \end{bmatrix} \tag{23}$$

where $\mathbf{I}_{i\times i} \in \mathbb{R}^{i\times i}$ is the identity matrix and $\mathbf{0}_{i\times j} \in \mathbb{R}^{i\times j}$ is a matrix with all the elements equal to zero.

Theorem 1: Let $\tilde{K}$ be the LQR gain of (21) with $\tilde{Q} = \mathrm{blkdiag}(Q, \mathbf{0}_{\Delta m\times \Delta m})$ and $\tilde{R} = R$ being the state and input weighting matrices, respectively. Then

$$\tilde{K} = K[A^{\Delta-1} \quad A^{\Delta-2}B \quad A^{\Delta-3}B \quad \cdots \quad B] \tag{24}$$

where K is the LQR gain for system (21) with $\Delta = 0$ and weighiting matrices Q and R, i.e.,

$$K = -\left(B^TSB+R\right)^{-1}B^TSA \tag{25}$$

$$S = A\left(S - SB(B^TSB+R)^{-1}B^TS\right)A + Q. \tag{26}$$

Proof: The optimal control law for system (21) is

$$u(k) = \tilde{K}x(k), \quad k \geq \Delta \tag{27}$$

where

$$\tilde{K} = -\left(\tilde{B}^T\tilde{S}\tilde{B}+\tilde{R}\right)^{-1}\tilde{B}^TS\tilde{A} \tag{28}$$

$$\tilde{S} = \tilde{A}\left(\tilde{S} - \tilde{S}\tilde{B}(\tilde{B}^T\tilde{S}\tilde{B}+\tilde{R})^{-1}\tilde{B}^T\tilde{S}\right)\tilde{A} + \tilde{Q}. \tag{29}$$

Partition the matrix $\tilde{S}$ according to the structure of the matrix $\tilde{A}$

$$\tilde{S} = \begin{bmatrix} S_{11} & S_{12} & S_{13} & \cdots & S_{1\Delta} \\ S_{21} & S_{22} & S_{23} & \cdots & S_{2\Delta} \\ \vdots & \vdots & \vdots & \vdots & \vdots \\ S_{\Delta 1} & S_{\Delta 2} & S_{\Delta 3} & \cdots & S_{\Delta\Delta} \end{bmatrix} \tag{30}$$

where $S_{11} \in \mathbb{R}^{n\times n}$, $S_{1j} \in \mathbb{R}^{n\times m}$, $j = 2, \ldots, \Delta$, $S_{i1} \in \mathbb{R}^{m\times n}$; $i = 2, \ldots, \Delta$, $S_{ij} \in \mathbb{R}^{m\times m}$, $i, j = 2, \ldots, \Delta$. By using the form (30) of $\tilde{S}$ and (23), the LQR gain $\tilde{K}$ in (28) can be written as

$$\tilde{K} = (S_{\Delta\Delta}+R)^{-1}\left[S_{\Delta 1}A \;\; S_{\Delta 1}B \;\; S_{\Delta 2}B \;\; \cdots \;\; S_{\Delta(\Delta-1)}B\right]. \tag{31}$$

It is immediate to prove by substitution that the Riccati equation (29) of the augmented system is solved by the following equations:

$$S_{1,1} = A^{T^{\Delta-1}}SA^{\Delta-1} + \sum_{k=1}^{\Delta-1} A^{T^{\Delta-1-k}}QA^{\Delta-1-k} + Q \tag{32}$$

$$S_{i,1} = B^TA^{T^{\Delta-i}}SA^{\Delta-1} + B^T\sum_{k=1}^{\Delta-i} A^{T^{\Delta-i-k}}QA^{\Delta-1-k}, \quad i = 2, \ldots, \Delta \tag{33}$$

$$S_{i,j} = B^TA^{T^{\Delta-i}}SA^{\Delta-1}B + B^T\left(\sum_{k=1}^{\Delta-i} A^{T^{\Delta-i-k}}QA^{\Delta-j-k}\right)B, \quad i = 2, \ldots, \Delta, \; j \leq i. \tag{34}$$

Equation (31) together with (32)–(34) prove the theorem. □

ACKNOWLEDGMENT

The authors would like to thank Prof. M. Morari for his helpful comments on a preliminary version of the manuscript. They would also like to thank A. Alessio for helping with the development of the C code for the explicit hybrid MPC algorithm based on quadratic costs.

REFERENCES

[1] A. T. Ander, D. Hrovat, C. J. Simonds, and L. F. Chen, "Vehicular surface traction characteristics estimation techniques," U.S. Patent 5 563 792, Oct. 8, 1996.

[2] R. Balakrishna and A. Ghosal, "Modeling of slip for wheeled mobile robots," *IEEE Trans. Robot. Autom.*, vol. 11, no. 1, pp. 349–370, Feb. 1995.

[3] M. Bauer and M. Tomizuka, "Fuzzy logic traction controllers and their effect on longitudinal vehicle platoon," *Veh. Syst. Dyn.*, vol. 25, no. 4, pp. 277–303, Apr. 1996.

[4] A. Bellini, A. Bemporad, E. Franchi, N. Manaresi, R. Rovatti, and G. Torrini, "Analog fuzzy implementation of a vehicle traction sliding-mode control," in *Proc. ISATA 29th Int. Symp. Automo. Technol. Auto.*, 1996, pp. 275–282.

[5] A. Bemporad. (2003, Dec.) *Hybrid Toolbox—User's Guide* [Online]. http://www.dii.unisi.it/hybrid/toolbox

[6] A. Bemporad, F. Borrelli, and M. Morari, "Piecewise linear optimal controllers for hybrid systems," in *Proc. Amer. Control Conf.*, 2000, pp. 1190–1194.

[7] A. Bemporad, A. Garulli, S. Paoletti, and A. Vicino, "Data classification and parameter estimation for the identification of piecewise affine models," in *Proc. 43th IEEE Conf. Decision Control*, 2004, pp. 20–25.

[8] A. Bemporad, N. Giorgetti, I. V. Kolmanovsky, and D. Hrovat, "A hybrid system approach to modeling and optimal control of DISC engines," in *Proc. 41th IEEE Conf. Decision Control*, 2002, pp. 1582–1587.

[9] A. Bemporad and M. Morari, "Control of systems integrating logic, dynamics, and constraints," *Automatica*, vol. 35, no. 3, pp. 407–427, Mar. 1999.

[10] A. Bemporad, M. Morari, V. Dua, and E. N. Pistikopoulos, "The explicit linear quadratic regulator for constrained systems," *Automatica*, vol. 38, no. 1, pp. 3–20, 2002.

[11] F. Borrelli, *Constrained Optimal Control of Linear and Hybrid Systems*. Berlin, Germany: Springer, 2003, vol. 290, Lecture Notes in Control and Information Sciences.

[12] F. Borrelli, M. Baotic, A. Bemporad, and M. Morari, "Dynamic programming for constrained optimal control of discrete-time hybrid systems," *Automatica*, vol. 41, no. 1, pp. 1709–1721, Jan. 2005.

[13] F. Borrelli, A. Bemporad, M. Fodor, and D. Hrovat, "A hybrid approach to traction control," in *Hybrid Systems: Computation and Control*, A. Sangiovanni-Vincentelli and M. D. Di Benedetto, Eds. Berlin, Germany: Springer-Verlag, 2001, Lecture Notes in Computer Science.
[14] T. M. Cavalier, P. M. Pardalos, and A. L. Soyster, "Modeling and integer programming techniques applied to propositional calculus," *Comput. Oper. Res.*, vol. 17, no. 6, pp. 561–570, 1990.
[15] V. Dua and E. N. Pistikopoulos, "An algorithm for the solution of multiparametric mixed integer linear programming problems," *Ann. Oper. Res.*, vol. 99, pp. 123–139, 2000.
[16] G. Ferrari-Trecate, M. Muselli, D. Liberati, and M. Morari, "A clustering technique for the identification of piecewise affine systems," in *Proc. 4th Int. Workshop Hybrid Systems: Computation Control*, vol. 2034, Lecture Notes in Computer Science, M. Di Benedetto and A. Sangiovanni-Vincentelli, Eds., 2001, pp. 218–231.
[17] M. Fodor, J. Yester, and D. Hrovat, "Active control of vehicle dynamics," in *Proc. 17th Dig. Avionics Syst. Conf.*, 1998, pp. 114/1–114/8.
[18] F. Gustafsson, "Slip-based tire-road friction estimation," *Automatica*, vol. 33, no. 6, pp. 1087–1099, 1997.
[19] D. Hrovat, J. Asgari, and M. Fodor, "Automotive mechatronic systems," in *Mechatronic Systems Techniques and Applications Volume 2—Transportation and Vehicular Systems*, C. T. Leondes, Ed. New York: Gordon and Breach, 2000, ch. 1.
[20] D. Hrovat and L. F. Chen, "Robust torque estimation using multitude of models," U.S. Patent 5 452 207, Sep. 19, 1995.
[21] P. Kachroo and M. Tomizuka, "An adaptive sliding mode vehicle traction controller design," in *Proc. IEEE Int. Conf. Syst., Man Cybernetics—Intelligent Syst. 21st Century*, vol. 1, 1995, pp. 777–782.
[22] G. F. Mauer, "A fuzzy logic controller for an ABS braking system," *IEEE Trans. Fuzzy Syst.*, vol. 3, no. 4, pp. 381–388, Nov. 1995.
[23] D. Q. Mayne, J. B. Rawlings, C. V. Rao, and P. O. M. Scokaert, "Constrained model predictive control: Stability and optimality," *Automatica*, vol. 36, no. 6, pp. 789–814, Jun. 2000.
[24] R. Raman and I. E. Grossmann, "Relation between MILP modeling and logical inference for chemical process synthesis," *Comput. Chem. Eng.*, vol. 15, no. 2, pp. 73–84, 1991.
[25] H. S. Tan, "Adaptive and robust controls with application to vehicle traction control," Ph.D. dissertation, Univ. California, Berkeley, CA, 1988.
[26] H. S. Tan and M. Tomizuka, "An adaptive sliding mode vehicle traction controller design," in *Proc. Amer. Control Conf.*, vol. 2, 1990, pp. 1856–1861.
[27] ——, "Discrete time controller design for robust vehicle traction," *IEEE Contr. Syst. Mag.*, vol. 10, no. 3, pp. 107–113, Apr. 1990.
[28] P. Tøndel, T. A. Johansen, and A. Bemporad, "Evaluation of piecewise affine control via binary search tree," *Automatica*, vol. 39, no. 5, pp. 945–950, May 2003.
[29] F. D. Torrisi and A. Bemporad, "HYSDEL—A tool for generating computational hybrid models," *IEEE Trans. Contr. Syst. Technol.*, vol. 12, no. 2, pp. 235–249, Mar. 2004.
[30] H. P. Williams, *Model Building in Mathematical Programming*, 3rd ed. New York: Wiley, 1993.

Francesco Borrelli received the Laurea degree in computer science engineering from the University of Naples Federico II, Naples, Italy, in 1998, and the Ph.D. degree from the Automatic Control Laboratory, ETH-Zurich, Zurich, Switzerland, in 2002.

He has been a Research Assistant with the Automatic Control Laboratory and a Contract Assistant Professor in the Aerospace and Mechanics Department, University of Minnesota, Minneapolis. He is currently an Assistant Professor at the Università del Sannio, Benevento, Italy. He is author of *Constrained Optimal Control of Linear and Hybrid Systems* (Springer Verlag, 2003). His research interests include constrained optimal control, model predictive control, robust control, parametric programming, singularly perturbed systems, and automotive applications of automatic control.

He received the Innovation Prize 2004 from the ElectroSwiss Foundation.

Alberto Bemporad received the M.S. degree in electrical engineering and the Ph.D. degree in control engineering from the University of Florence, Florence, Italy, in 1993 and 1997, respectively.

He spent the academic year 1996–1997 with the Center for Robotics and Automation, Department of Systems Science and Mathematics, Washington University, St. Louis, as a Visiting Researcher. In 1997–1999, he held a postdoctoral position with the Automatic Control Lab, ETH-Zurich, Zurich, Switzerland, where he collaborated as a Senior Researcher in 2000–2002. In 1999, he became an Assistant Professor in the Faculty of Engineering, University of Siena, Siena, Italy, where he has been an Associate Professor since 2005. He has published several papers in the area of hybrid systems, model predictive control, multiparametric optimization, computational geometry, robotics, and automotive control. He is coauthor of the *Model Predictive Control Toolbox* (The Mathworks, Inc.) and author of the *Hybrid Toolbox for Matlab*.

Prof. Bemporad was an Associate Editor of the IEEE TRANSACTIONS ON AUTOMATIC CONTROL during 2001–2004. He has been Chair of the Technical Committee on Hybrid Systems of the IEEE Control Systems Society since 2002.

Michael Fodor received the B.S. degree in mechanical engineering from the University of Oklahoma, Norman, in 1990, and the M.S. degree in mechanical engineering from Texas A&M University, College Station, in 1993.

He has since been with Ford Motor Company Research Laboratories, Dearborn, MI, working in the area of vehicle dynamic and powertrain modeling and controls, where he currently is a Technical Expert.

Davor Hrovat received the Dipl. Ing. degree from the University of Zagreb, Croatia, in 1972, and the M.S. and Ph.D. degrees in mechanical engineering from the University of California, Davis, in 1976 and 1979, respectfully.

Since 1981, he has been with Ford Motor Company Research Laboratories, Dearborn, MI, where he is a Corporate Technical Specialist coordinating and leading research efforts on various aspects of vehicle/power train control systems. He has received numerous patents. He has served as an Associate Editor for the ASME *Journal of Dynamic Systems, Measurement and Control* and the ASME *Applied Mechanics Review*. He is currently an Editor for the IFAC journal *Control Engineering Practice,* the *International Journal of Vehicle Autonomous Systems,* and *Vehicle System Dynamics*.

Dr. Hrovat is a Fellow of the American Society of Mechanical Engineers (ASME). He has served on the Board of Editors for *IEEE Control Systems Magazine*. He received the 1996 ASME/Dynamic Systems and Control Innovative Practice Award and the 1999 AACC Control Engineering Practice Award.

Erratum

In the May 2006 issue of the IEEE TRANSACTIONS ON CONTROL SYSTEMS TECHNOLOGY, the paper entitled "An MPC/Hybrid System Approach to Traction Control" by F. Borrelli, A. Bemporad, M. Fodor, and D. Hrovat should have been listed in the "Papers" section on the Table of Contents [1]. It was inadvertently included among Brief Papers. IEEE regrets the error.

REFERENCES

[1] *IEEE Trans. Control Syst. Technol.*, vol. 14, no. 3, pp. 541–552, May 2006.

Manuscript received May 30, 2006.
Digital Object Identifier 10.1109/TCST.2006.878279